JMEPEG (2015) 24:1079–1085
DOI: 10.1007/s11665-014-1365-1

1059-9495/$19.00

Influences of High-Temperature Diffusion on the Homogenization and High-Temperature Fracture Behavior of 30Cr1Mo1V

Xingang Liu, Dongning Meng, Yuhui Wang, Huan Chen, and Miao Jin

(Submitted June 18, 2014; in revised form November 27, 2014; published online December 24, 2014)

High-temperature diffusion is an important process for manufacture of 30Cr1Mo1V rotor steel to alleviate the dendritic segregation and improve the hot workability of the steel ingots. However, the functions and significances of high-temperature diffusion in heavy forging production are still academically controversial. This paper investigated the influences of high-temperature diffusion on the homogenization of dendritic segregation and dendritic structure of 30Cr1Mo1V. After the samples being treated under different high-temperature diffusion process, hot stretch experiments have been performed to study the influences of high-temperature diffusion on the flow stress and the fracture behavior. The results reveal that after being held at high temperature for a long period of time, the segregation ratios of Mo element were greatly reduced and no dendritic structure can be observed by optical microscopy. The percent reduction in the area and the fracture limit increases as temperature increases. Moreover, high-temperature diffusion has less influences on the flow stress while, at different temperature ranges, the influences on fracture limit differ considerably.

Keywords 30Cr1Mo1V steel, fracture behavior, high-temperature diffusion, high-temperature tensile

1. Introduction

Based on 30Cr2MoV steel, 30Cr1Mo1V steel is achieved by lowering the Cr weight percentage while increasing that of Mo. It has excellent high-temperature mechanical performance (Ref 1, 2) and is widely used in manufacturing high and intermediate pressure rotors for the large fossil-fuel power units (Ref 3). However, it is relatively difficult to make 30Cr1Mo1V rotor forgings for the manufacture process is complicated.

Recently, much attention has been paid on 30Cr1Mo1V steel's performance in service. Seok and Kim (Ref 4) studied the mechanical properties of 30Cr1Mo1V steel in service. In their study, samples were taken from four thermally aged areas to carry out the ultrasonic tests, tensile tests, toughness tests, and hardness tests. Comparison and analysis of the results showed that the ultrasonic tests were able to evaluate the mechanical properties of 30Cr1Mo1V more accurately. Wilshire and Scharning (Ref 5) found that the crystalline fracture modes and the micro-structural evolution of the tempered Bainite changed in the creep experiments, and an effective method has also been developed to predict and collect creep data of 30Cr1Mo1V steel, which can accurately predict its service life. Shekhter et al. (Ref 6) measured the fracture toughness of 30Cr1Mo1V steel using three different impact toughness tests (Charpy V-Notch test, small punch test and full size K_{IC} test) and investigated the remaining fatigue life, finally drew the conclusion that small punch test can get better results. Kulvir and Kamaraj (Ref 7) conducted high-temperature tests on the 30Cr1Mo1V forgings and castings. They comparatively analyzed the third stage of the creep deformations and the creep ductility of its forgings and castings. Evans (Ref 8) normalized the Wilshire-Scharning model predicting long-term creep life. The normalized model not only increased the success rate of the creep life predicting experiments of 30Cr1Mo1V steel, but also can be applied to any other materials. However, the hot workability of 30Cr1Mo1V steel has been rarely studied.

High-temperature diffusion is an important procedure for manufacturing 30Cr1Mo1V rotor forgings, by which the dendritic segregation of the ingot can be reduced (Ref 9) and the hot workability can be improved. Although high-temperature diffusion has been used on producing the heavy forging for a long time, many controversies still exist. Many researchers have studied the high-temperature diffusion process on various materials (Ref 10-14), however, to the best of our knowledge, the influences of high-temperature diffusion on 30Cr1Mo1V steel and its hot workability have never been investigated systematically.

2. Experimental Materials and Method

A 3-ton 30Cr1Mo1V ingot poured in natural atmosphere is used in this study. Analysis shows the chemical composition of the ingot is (wt.%): C = 0.30, Mn = 0.79, Si = 0.22, Cr = 1.13, Mo = 1.17, V = 0.26, P = 0.005, and S = 0.002.

Several 15 mm × 15 mm × 5 mm specimens were taken from the columnar crystal region of the ingot. The specimens were

Xingang Liu, Dongning Meng, Huan Chen, and **Miao Jin**, College of Mechanical Engineering, Yanshan University, Qinhuangdao, 066004 Hebei, China; and **Yuhui Wang**, National Engineering Research Center for Equipment and Technology of Cold Strip Rolling, College of Mechanical Engineering, Yanshan University, Qinhuangdao, 066004 Hebei, China. Contact e-mail: lxg@ysu.edu.cn.

grinded, polished, and finally etched in the heated supersaturated picric acid solution, and then their dendritic structures were observed by scanning electron microscopy (SEM). Both the dendrite arm and the interdendritic regions can be clearly identified. After being heated, the as-cast dendrites are very difficult to be observed in the metallographs. The specimen surface was carefully polished before electron probe microanalyzer (EPMA) test to find the dendrites. The dendrites were marked after specimens etching using the microhardness point method, and the distance of microhardness point goes across two secondary dendrite arms.

The specimens were heated inside a vacuumed quartz tube. Before the tube was sealed, the inner wall of the tube was cleaned by HF solution. The surface of the specimen was cleaned by HF solution as well before the compositions of the specimen were analyzed. When the specimen was ready, EPMA-1720 was used to carry out the composition analysis. For every specimen, 20 different lines (each line across two secondary dendrite arms) were scanned for further analyses.

The specimens were treated under three different conditions: one was the as-cast specimen without further heat treatment; the other two were heated to 1200 °C and then held for 20 h and 40 h, respectively, and finally air cooled down to room temperature. The processed specimens were turned into cylinders with the height of 110 mm, as shown in Fig. 1. The l_1 section is threaded with a length of 10 mm, with which the specimen fits with a nut of M10. The 30 mm l_2 section fits with a dedicated Gleeble-3500 fixture block. The l_3 is a free span of 30 mm long.

The tensile tests were carried out on a Gleeble-3500 thermo-mechanical simulator. The procedure was: the specimen was first heated to the deformation temperature at a heating rate of 20 °C/s and held for 15 s; then it was elongated at a stroke speed of 50 mm/s until it was broken. The tensile deformation temperatures were 850, 950, 1050, 1150, and 1250 °C, respectively. Through the built-in data collecting system on the Gleeble thermo-mechanical simulator, the load, displacement, and temperature etc. were recorded during the deformation process. Finally, the true stress-strain curves of the 30Cr1Mo1V steel at different conditions were acquired. The fracture surfaces were characterized by SEM.

3. Experimental Results and Analysis

3.1 Homogenization of Alloy Elements

Figure 2 shows the as-cast dendritic structures of the specimens. It can be seen that there are obvious dendritic structures existing in the tested materials. The primary dendritic arms, secondary dendritic arms, and the interdendritic regions are clearly observed, indicating that the average spacing (l) between the adjacent secondary dendrite arms is 83 μm (0.0083 cm).

Figure 3 shows a typical element distribution curve of Cr, Mo, and V measured using EPMA line scanning on the as-cast 30Cr1Mo1V, which is perpendicular to secondary dendrite arm. In order to exhibit the obtained data clearly, a baseline has been subtracted from each distribution curve, making the minimum values in three curves overlapped. It can be seen that the concentration distribution of the alloy elements periodically changes along the secondary dendrite arm, and the concentrations of Cr, Mo, and V in the interdendritic regions are apparently higher than those in the dendrite arm. The segregation ratio (SR) representing the inhomogeneity degree of composition distribution is defined as

$$\mathrm{SR} = \frac{c_{\max}}{c_{\min}} \qquad \text{(Eq 1)}$$

where $c_{\max}$ is the maximum concentration of the alloy elements in the interdendritic regions and $c_{\min}$ is the corresponding minimum concentration. The Interdendritic and dendrite arm regions of the specimens are scanned by EMPA in the point mode. 20 different lines (each line across two dendrite arms) were scanned and used to calculate the corresponding SR, and then the average value was obtained. The averaged SR of Cr element in the as-cast 30Cr1Mo1V is 1.048, Mo element is 1.344 and V element is 1.223. Therefore, the SR of Cr element is lower than those of Mo and V.

After high-temperature diffusion at 1200 °C for 10 h, the element concentration of the alloy in the interdendritic regions decreases, and Mo element shows the biggest change. The SR of Cr, Mo, and V elements is reduced to 1.041, 1.119, and 1.208, respectively. In the as-cast 30Cr1Mo1V, the degree of segregation of Cr element is relatively low, therefore, the SR of Cr element shows only a slight decrease after high-temperature diffusion. Meanwhile, the SR of V element also decreases slightly, only about 1%.

As the decrease of the SR of Mo element is more remarkable than those of other elements, here we further discuss the composition homogenization of Mo element. The unsteady state diffusion can be expressed by Fick-2 Law

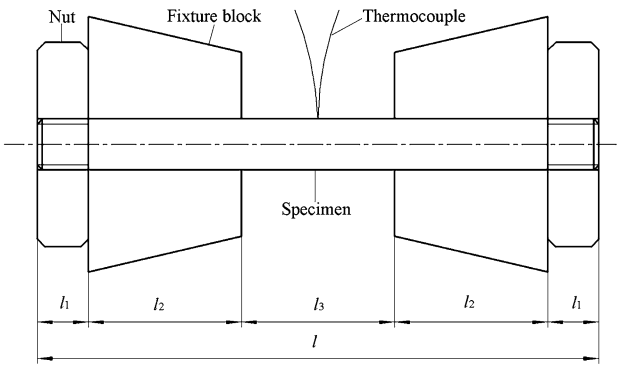

Fig. 1 Sketch of a specimen for the tensile test

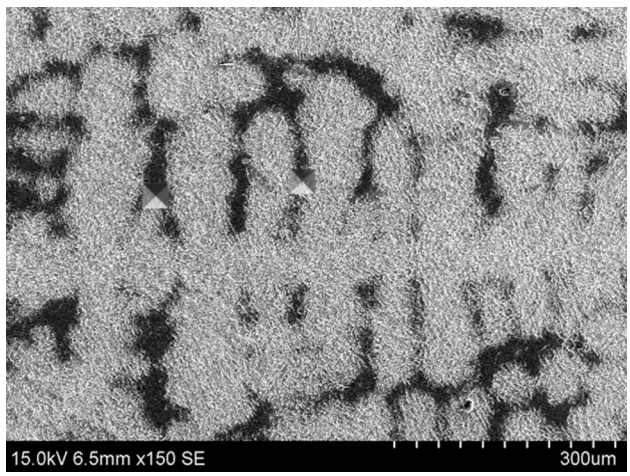

Fig. 2 As-cast dendritic structures in 30Cr1Mo1V

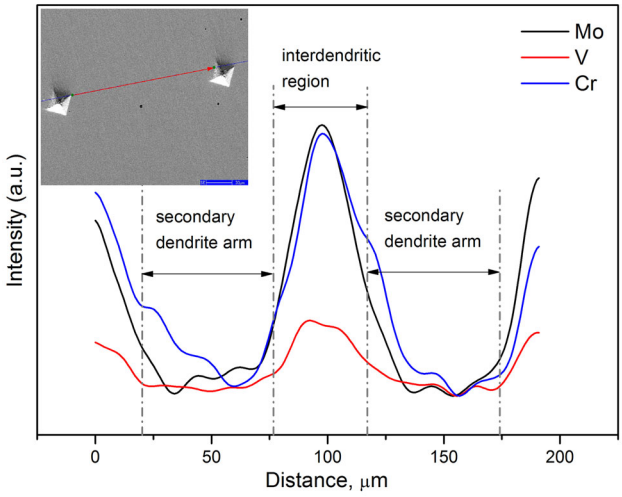

Fig. 3 Element distribution curves of the as-cast 30Cr1Mo1V

$$\frac{\partial C}{\partial t} = D\frac{\partial^2 C}{\partial x^2} \qquad \text{(Eq 2)}$$

where D is the diffusion coefficient, C is the solute concentration, t is the holding time, and x is the distance. There are many different solutions for Eq 2. When dealing with the homogenization of compositions of the casting alloys in hot working processes, Shewmon (Ref 15) expressed the solutions of diffusion problems in a cosine form

$$C(x,t) = c_0 + c_m \cos\frac{\pi x}{l}\exp\left(-\frac{\pi^2 Dt}{l^2}\right). \qquad \text{(Eq 3)}$$

This expression not only conforms to the Fick-2 law equation, but also reflects the periodic distribution of the secondary dendrite arm of the alloy elements in the dendritic segregation. Hence, this model has been widely used. However, the concentrations of the alloy elements in the dendrite not only show a periodic distribution, but the concentration gradient of the area near the maximum value is much larger than the area near the minimum value. This characteristic agrees with the calculated results from the model for the solute redistribution of the alloys (Ref 16), as well as the experimental results reported by Hone et al. (Ref 17). To solve this problem, Zhang (Ref 18) developed a dendritic segregation model based on Gauss solution, in which the concentration of the alloy elements in the dendrite can be expressed as

$$C(x,t) = \frac{S}{\sqrt{\pi \cdot 4Dt}} \cdot \sum_{i=0}^{n} \exp\frac{-(x \pm il)^2}{4Dt}, \qquad \text{(Eq 4)}$$

where l is the spacing between the adjacent secondary dendrite arms. When $t = 0$, Eq 4 describes the alloy elements gathering at the points of $x = 0$, $\pm l$, $\pm 2l$,…, $\pm nl$, and the total of the element atoms at every point atom is S. Obviously, at the beginning of high-temperature diffusion, the concentration distribution of the alloy elements is different from that described by Eq 4 at $t = 0$. However, there must be a t ($t = t'$), at which the equation fits the curve of the concentration as shown in Fig. 3. Then, the concentration at the diffusion time t' can be considered as the initial concentration of the homogenization of dendritic segregation. It can be described as

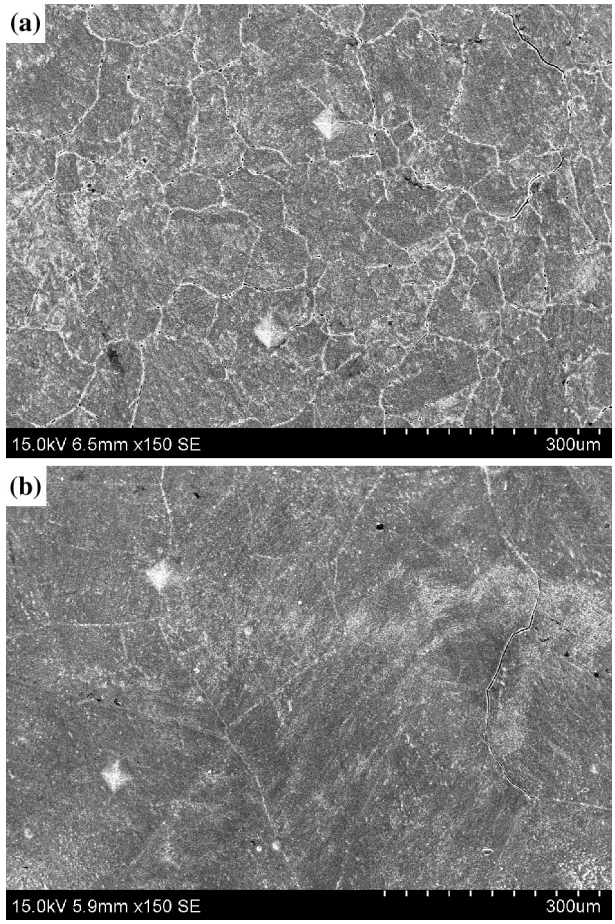

Fig. 4 SEM metallographs after different holding times of diffusion at 1200 °C. (a) 20 h, (b) 40 h

$$C(x,0) = \frac{S}{\sqrt{\pi 4Dt'}} \cdot \sum_{i=0}^{n} \exp\frac{-(x \pm il)^2}{4Dt'} \qquad \text{(Eq 5)}$$

After the diffusion time t', the function follows the expression

$$C(x,t) = \frac{S}{\sqrt{\pi 4D(t+t')}} \cdot \sum_{i=0}^{n} \exp\frac{-(x \pm il)^2}{4D(t+t')} \qquad \text{(Eq 6)}$$

when $n \to \infty$, Eq 6 reaches the maximum value with $x = 0$, $\pm l$, $\pm 2l$,…, and reaches the minimum value with $x = \pm 12l$, $\pm 32l, \cdots$. Thus, the SR is

$$\mathrm{SR} = \frac{c_{\max}}{c_{\min}} = \frac{C(0,t)}{C(\frac{1}{2}l,t)} = \frac{\sum_{i=0}^{n} \exp\frac{-(\pm il)^2}{4D(t+t')}}{\sum_{i=0}^{n} \exp\frac{-(\frac{1}{2}l \pm il)^2}{4D(t+t')}} \qquad \text{(Eq 7)}$$

We approximately consider that the maximum concentration $c_{\max}$ at $x = 0$ is related to the diffusion process of the original accumulation of atoms at $x = 0$ and $x = \pm l$. Due to the long distance of other diffusion sources, their contribution can be ignored. The similar process can also be used for obtaining $c_{\min}$. When $n = 1$, Eq 7 can be expressed as (Ref 19)

$$\mathrm{SR} = \frac{1 + 2 \cdot \exp\frac{-l^2}{4D(t+t')}}{2 \cdot \exp\frac{-\frac{1}{4}l^2}{4D(t+t')} + \exp\frac{-\frac{9}{4}l^2}{4D(t+t')}} \qquad \text{(Eq 8)}$$

Based on the testing results, when $t = 0$, the SR of Mo element is 1.344. After the diffusion process at 1200 °C for 10 h, the SR of Mo element reduces to 1.119. By substituting the obtained value of $l = 0.0083$ cm into Eq 8, we can obtain the diffusion coefficient of Mo element at 1200 °C: $D = 4.74 \times 10^{-11}$ cm^2/s and $t' = 96200$ s. Therefore, the change of the SR of Mo during the holding time in 30Cr1Mo1V at 1200 °C can be expressed as

$$\mathrm{SR} = \frac{1 + 2 \cdot \exp\frac{-1.45\times10^6}{t+96200}}{2 \cdot \exp\frac{-3.63\times10^5}{t+96200} + \exp\frac{-3.27\times10^6}{t+96200}}. \quad \text{(Eq 9)}$$

The calculated SR of Mo element reduces to 1.049 and 1.027 after high-temperature diffusion at 1200 °C for 20 and 40 h, respectively. In this case, the segregation of the alloy elements in the dendritic structures of 30Cr1Mo1V decreased greatly, so that it is difficult to observe the dendrite morphology in the etched specimen, as shown in Fig. 4.

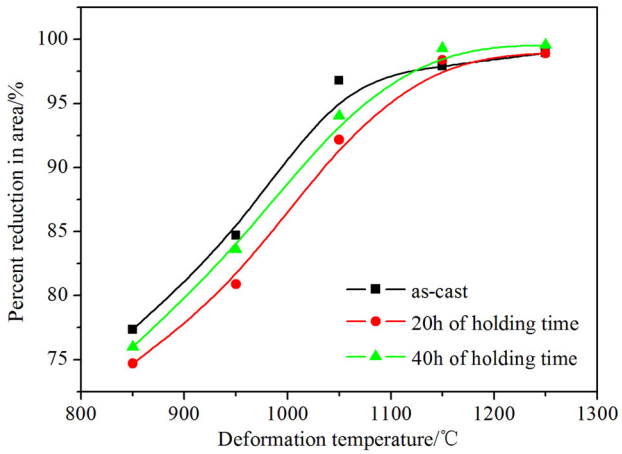

Fig. 5 Relationship between percent reduction in area and deformation temperature

3.2 Thermoplasticity

Figure 5 shows the percent reduction in the area (Ψ)-deformation temperature curves at different holding times. It indicates that Ψ increases as the deformation increases, no matter whether high-temperature diffusion is done for the 30Cr1Mo1V steel or not. Within the temperature range of 850-1250 °C, for the as-cast specimens and those after diffusion for 20 and 40 h, the percent reductions in the area (Ψ) increase from 77.34, 74.70, and 75.99 to 98.94, 98.90, and 99.54%, respectively.

The tensile tests performed at 850-1050 °C demonstrate that the percent reductions in the area of the specimens without further treatment are higher than those of the specimens after high-temperature diffusion for both 20 and 40 h. While at 1150-1250 °C, all the processed specimens have basically same

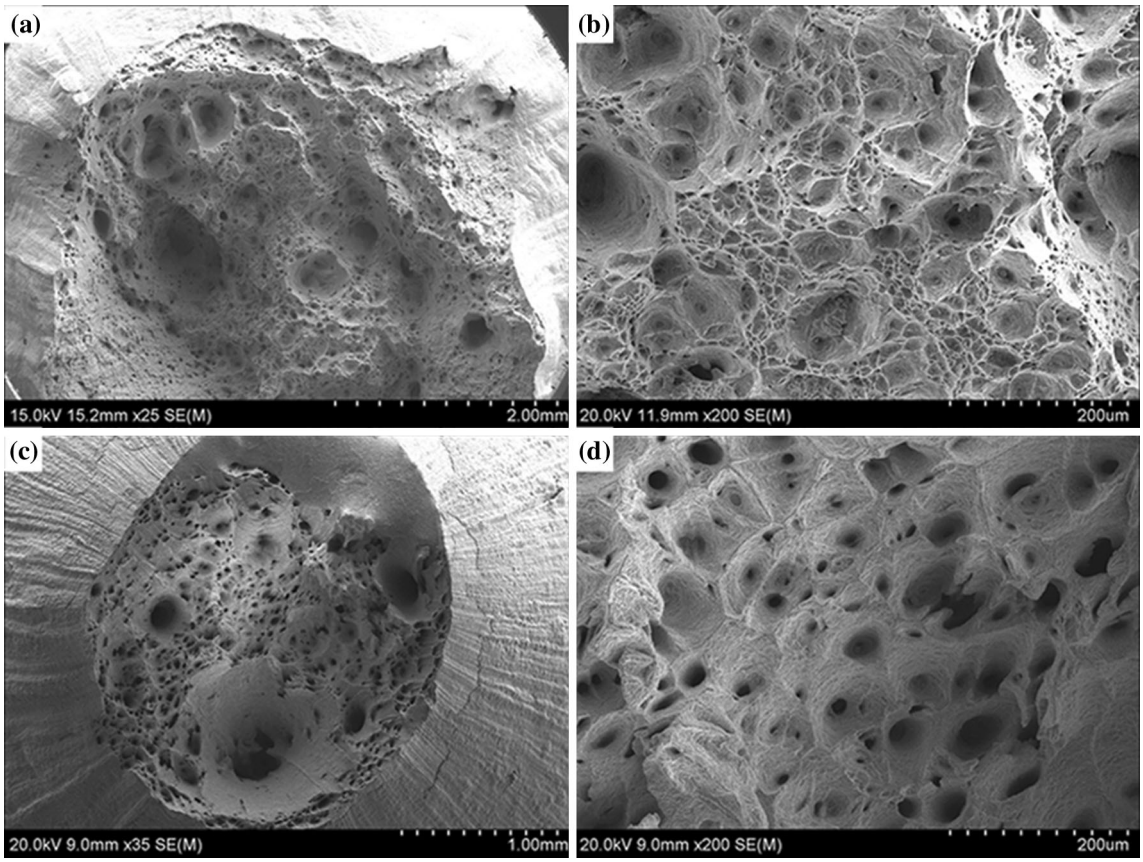

Fig. 6 Fracture surfaces at different temperatures. (a) 850 °C; (b) 850 °C; (c) 1050 °C; and (d) 1050 °C

Ψ. This is to say, at lower temperatures (850-1050 °C), the high-temperature diffusion process does not exhibit positive effect on the thermoplasticity of 30Cr1Mo1V steel, this is because the grain size has an important influence on the reduction of the area, and the grain size in the specimens after the high-temperature diffusion treatment is larger than that in as-cast specimen. While at higher testing temperatures (1150-1250 °C), the high-temperature diffusion process, to a certain degree, improves the thermoplasticity of 30Cr1Mo1V steel owing to the decreasing of the segregation degree, because the high-temperature diffusion process has a significant effect on the reduction of the area.

Figure 6 shows SEM metallographs of the fracture surfaces at different testing temperatures. Cup-shaped macro-fracture has been observed in the fracture surfaces of 30Cr1Mo1V at 850 °C (Fig. 6a and b) and 1050 °C (Fig. 6c and d) after holding for 20 h. But at the testing temperature higher than 1050 °C, the densely and evenly distributed dimples with good plasticity can be clearly observed.

3.3 High-Temperature Tensile Stress Curve and Fracture Limit

As shown in Fig. 7, at the same deformation temperature, the stress increases rapidly as the strain increases. When the stress exceeds the yield strength, homogeneous plastic deformation occurs first. The stress increases to its maximum at a certain strain, and then begin to decrease when the strain continues to increase. The specimen is subject to the inhomogeneous plastic deformation and the necking takes place. With more and more crack developed, the specimen is finally fractured. At 1050 °C, the peak stress of the specimen holding for 40 h is 10.79 MPa lower than that of the as-cast specimen (Fig. 7a). While at 1250 °C, as shown in Fig. 7(b), the peak stress of specimens after holding for 40 h and 20 h is 5.41 and 4.76 MPa, respectively, higher than that of the as-cast specimen, respectively.

Figure 8 indicates at high temperatures, the peak stress decreases quickly as the deformation temperature increases. But at the same temperature, there are a few differences from the peak stress of the specimens treated by different high-temperature diffusion processes, which means high-temperature diffusion have slight influences on the peak stress.

High-temperature fracture limit of metals, C, is an important physical quantity to evaluate the hot formability and the brittle failure resistance of metals. Normalized Cockcroft and Latham fracture criterion considers the fracture at constant deformation temperature and strain rate, and the metal fractures when the tensile stress-strain energy reaches a critical damage value (Ref 20). The fracture limit can be expressed as

$$\int_0^{\varepsilon_f} \frac{\sigma^*}{\bar{\sigma}} d\bar{\varepsilon} = C, \qquad \text{(Eq 10)}$$

where σ^* is the maximum tension stress when the metal fractures, which is equal to the maximum principal stress; ε_f is the fracture strain. Because during the hot stretch process, cracks mainly result from the strains in the stretching direction, the true stress ε_1 can be used as $\bar{\varepsilon}$ and the metal's ultimate tensile strength, as $\bar{\sigma}$. Therefore,

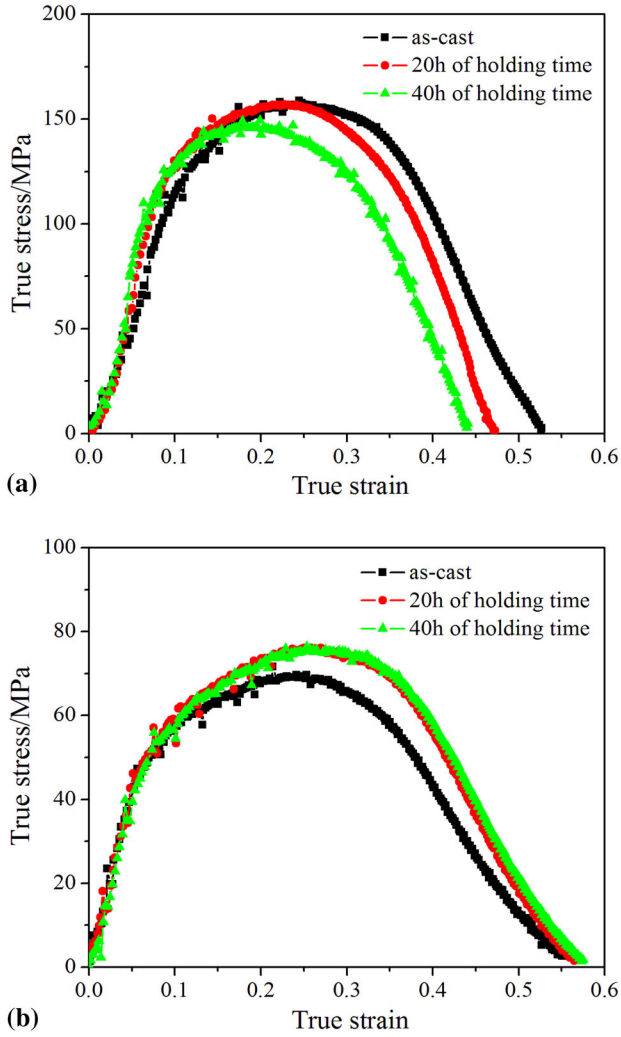

Fig. 7 True tensile stress-strain curves at different deformation temperatures. (a) 1050 °C (b) 1250 °C

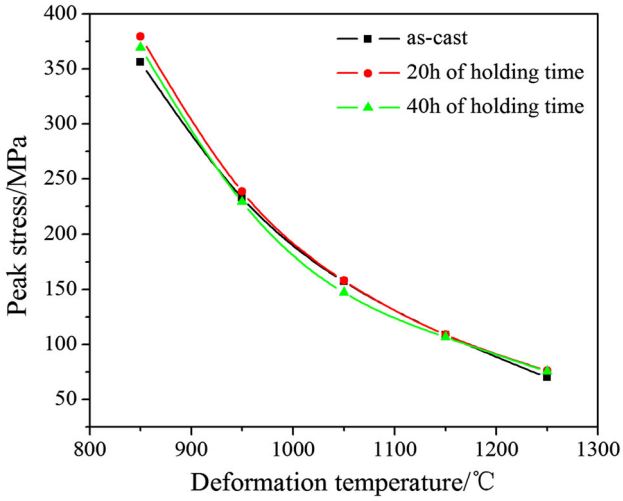

Fig. 8 Relationship between peak stress and deformation temperature

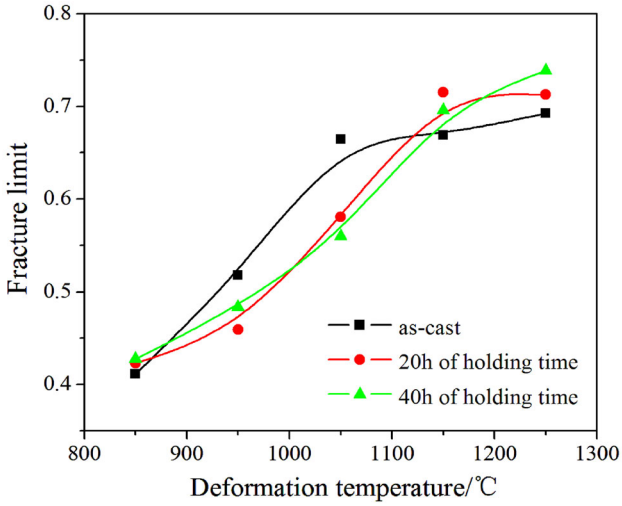

Fig. 9 Changes of fracture limit of the 30Cr1Mo1V with the deformation temperature after different high-temperature diffusion treatments

$$\int_0^{\varepsilon_f} \frac{\sigma_1}{\sigma_{UTS}} d\varepsilon_1 = C \qquad \text{(Eq 11)}$$

In Eq 11, the maximum principal σ_1, the material's ultimate tensile stress σ_{UTS}, and the true tensile strain ε_1, can be calculated from the stress-strain curves. Then, we have

$$C = \int_0^{\varepsilon_f} \frac{\sigma_1}{\sigma_{UTS}} d\varepsilon_1 = \left(\frac{\sigma_{limit}}{\sigma_{UTS}}\right) \cdot \varepsilon_{limit}, \qquad \text{(Eq 12)}$$

where σ_{limit} is the ultimate tensile stress, and ε_{limit} is the ultimate tensile strain.

Figure 9 shows curves depicting the change of the fracture limit with deformation temperature. It indicates that a higher deformation temperature is beneficial to increasing the fracture limit, C, of the 30Cr1Mo1V steel. Take the specimen with the holding time of 20 h as an example, the fracture limit is 0.42 at 850 °C while increases to 0.71 at 1250 °C. The higher fracture limit means a greatly improved forgeability. Therefore, increasing forging temperature allows much bigger deformations of the first several heatings of the 30Cr1Mo1V rotor steel forgings.

If the specimen is as-cast, after the deformation temperature reaches 1050 °C, the fracture limit hardly increases as the deformation temperature further increases. Whereas, the specimens with the holding time of 20 and 40 h, within the ranges of experiment parameters, their fracture limits continue to increase with the increase of the deformation temperature even higher than 1050 °C.

In addition, at lower temperatures (≤ 1050 °C), high-temperature diffusion cannot improve the fracture limit. At 950 and 1050 °C, the specimens treated by high-temperature diffusion display much smaller fracture limits than those without being treated, and this phenomenon can be attributed to the higher ductility of the as-cast specimen. At higher temperatures (≥ 1150 °C), the fracture limit of the specimens after high-temperature diffusion increases obviously, and this phenomenon is related to the peak stress of the specimens after high-temperature diffusion. Therefore, high-temperature diffusion before forging can greatly improve the forgability and the production efficiency of the 30Cr1Mo1V rotor steel's at high temperatures.

4. Conclusion

1. High-temperature diffusion greatly relieves the degree of segregation of the alloy elements in the 30Cr1Mo1V ingot.
2. High-temperature diffusion has quite small influence on the flow stress of the as-cast 30Cr1Mo1V at high temperature.
3. A high deformation temperature is beneficial to increasing the high-temperature plasticity and the fracture limit of the 30Cr1Mo1V steel. At lower deformation temperatures ($T \leq 1050$ °C), high-temperature diffusion only has a small influence on the high-temperature plasticity of 30Cr1Mo1V steel. While at high deformation temperatures ($T \geq 1150$ °C), high-temperature diffusion can improve the high-temperature plasticity and the fracture limit of 30Cr1Mo1V steel.

Acknowledgments

This work was supported by the National Natural Science Foundation of China (Grant No.: 51005198), Scientific and Technological Research Foundation for Outstanding Young Talents of Hebei provincial Universities (Grant No.: Y2012034) and College Innovation Team Leader Training Program of Hebei Province (Grant No.: LJRC012). In addition, the author also thanks Dr. Longjiang Niu for his help in language.

References

1. A. Joarder, D.S. Sarma, and N.S. Cheruvu, Effect of Long-Term Service Exposure on Microstructure and Mechanical Properties of a CrMoV Steam Turbine Rotor Steel, *Metall. Trans. A*, 1991, **22**(8), p 1811–1820
2. S.H. Nahm, Y.I. Kim, K.M. Yu, and A. Kim, Evalution of Fracture Toughness of Degraded Cr-Mo-V Steel Using Electrical Resistivity, *J. Mater. Sci.*, 2002, **37**(16), p 3549–3553
3. C.S. Seok and J.M. Koo, Evaluation of Material Degradation of 1Cr-1Mo-0.25V Steel by Non-destructive Method, *Mater. Sci. Eng. A*, 2005, **395**(1–2), p 141–147
4. C.S. Seok and J.P. Kim, Studies on the Correlation Between Mechanical Properties and Ultrasonic Parameters of Aging 1Cr-1Mo-0.25V Steel, *J. Mech. Sci. Technol.*, 2005, **19**(2), p 487–495
5. B. Wilshire and P.J. Scharning, Prediction of Long Term Creep Data for Forged 1Cr-1Mo-0.25V Steel, *Mater. Sci. Technol.*, 2008, **24**, p 1–9
6. A. Shekhter, S. Kim, D.G. Carr, A.B.L. Croker, and S.P. Ringer, Assessment of Temper Embrittlement in an Ex-service 1Cr-1Mo-0.25V Power Generating Rotor by Charpy V-Notch Testing, KIc Fracture Toughness and Small Punch Test, *Int. J. Press. Vessel Pip.*, 2002, **79**(8–10), p 611–615
7. S. Kulvir and M. Kamaraj, Creep Ductility of 1Cr-1Mo-0.25V Low Alloy Forging and Casting Steels, *Mater. Sci. Eng. A*, 2009, **510–511**, p 51–57
8. M. Evans, Formalisation of Wilshire-Scharning Methodology to Creep Life Prediction with Application to 1Cr-1Mo-0.25V Rotor Steel, *Mater. Sci. Technol.*, 2010, **26**, p 309–317
9. K.Y. Kwon, Y.S. Na, and S.M. Seo, Microstruetural Changes and Variations of Hot Deformation Stability with Homogenization Treatment of 1Cr-1.25Mo-0.25V Steel Before Hot Forging, Korean, *J Met. Mater.*, 2013, **51**(12), p 883–892
10. I.A. Borisov, Heat Treatment of Large Castings from Steel 15Kh3M1FTsL, *Met. Sci. Heat Treat.*, 2004, **46**(9–10), p 430–435
11. M. Torkar, F. Vodopivec, and S. Petovar, Analysis of Segregations in As-cast X40CrMoV51 Steel, *Mater. Sci. Eng. A*, 1993, **173**, p 313–316
12. R.W. Heckel and M. Balasubramaniam, The Effect of Heat Treatment and Deformation on the Homogenization of Compacts of Blended Powders, *Metall. Trans.*, 1971, **2**, p 379–391

13. G.S. Cole, Inhomogenization and Their Control Via Solidification, *Metall. Trans.*, 1971, **2**, p 357–370
14. J.C. Viala, N. Peillon, L. Clochefert, and J. Bouix, Diffusion Paths and Reaction Mechanisms in the High-Temperature Chemical Interaction Between Carbon and Titanium Aluminides, *Mater. Sci. Eng. A*, 1995, **203**(1–2), p 222–237
15. P.G. Shewmon, *Diffusion in Solids*, McGraw-Hill Book Co., New York, 1963, p 1–85
16. D.M. Xu, H.Z. Fu, J.J. Guo, J. Jia, and Q.C. Li, A Unified Model for Micro-scale Solute Redistribution in Dendrite Solidification of Alloys, *J. Harbin Inst. Technol.*, 2003, **35**(10), p 1156–1161
17. M. Hone, S.V. Subramanian, and G.R. Purdy, Estimating Terminal Phase Equilibria in Ternary Systems, *Can. Metall. Quart.*, 1969, **8**(3), p 251–256
18. D.F. Zhang and J. Peng, Diffusion Models for Solid-State Homogenization of Dendrite Segregation, *Mater. Sci. Ed.*, 2005, **20**(2), p 111–114
19. X.G. Liu, B. Liu, H. Guo, M. Jin, and B.F. Guo, Study on Mathematical Model of Homogenization of Dendritic Segregation, *Adv. Mater. Res.*, 2012, **430–432**, p 355–360
20. M.G. Cockcroft and D.J. Latham, Ductility and the Workability of Metals, *J. Inst. Met.*, 1968, **96**(2), p 33–39